Hole Localization and Thermochemistry of Oxidative Dehydrogenation of Aqueous Rutile TiO2(110)

Cheng, Jun ; Sulpizi, Marialore ; VandeVondele, Joost ; Sprik, Michiel

DOI: https://doi.org/10.1002/cctc.201100498

Hole Localization and Thermochemistry of Oxidative Dehydrogenation of Aqueous Rutile TiO_2(110)

Jun Cheng,[*,†] Marialore Sulpizi,[†,¶] Joost VandeVondele,[‡,§] and Michiel Sprik[†]

Department of Chemistry, University of Cambridge, Cambridge CB2 1EW, United Kingdom, and Physical Chemistry Institute, University of Zurich, Winterthurerstrasse 190, CH-8057 Zurich, Switzerland

E-mail: jc590@cam.ac.uk

Abstraction of an H atom, or oxidative dehydrogenation(ODH), is an energetically demanding process. The reversible potential for ODH of a water molecule ($H_2O \rightarrow OH^\bullet + \frac{1}{2}H_2$) is 2.72 V *vs* the standard hydrogen electrode (SHE). This is more than the double of the 1.23 V needed for the full four electron oxidation of H_2O. The extra energy must also be provided by the external force driving the reaction. In photoelectrochemical splitting this is the valence band hole generated by photo excitation. Photo-anodes must therefore have deep lying valence bands, which is why metal oxides are attractive materials for photo-catalytic water oxidation.[1] TiO_2 is historically one of the first metal oxides shown to be capable of evolving oxygen when exposed to light and has become the model photo-anode.[2] The valence band maximum (VBM) for the rutile form is 2.95 V in the dark and 3.25 V in the light *vs* SHE at pH = 0.[1] While exceeding the thermodynamic minimum, the TiO_2 VBM seems to leave surprisingly little margin for energy losses which can be expected if the localization of free holes is fast.[2]

In photo-catalytic water splitting the holes do not have to supply the full energy for ODH of H_2O in the liquid. It may be easier to eliminate hydrogen from an adsorbed water molecule with the product $OH^\bullet$ remaining as an intermediate on the surface. The question is therefore, how much energy is saved by adsorption. This energy is not directly available from experiment but has been computed for TiO_2 anodes using Density Functional Theory (DFT) methods.[3,4] The focus in these calculations was on electro-oxidation. Overpotentials for electrolysis can be estimated without explicit computation of the energy of holes (the same procedure has been applied to metallic oxides such as RuO_2[5,6]). In fact, because of shortcomings in the generalized gradient approximation (GGA) to the density functionals used in the calculations of Refs. 3,4 the question of localization of holes could not be addressed in principle.

Self trapping of holes in titania has been the subject of several recent computational investigations using advanced DFT techniques.[7–10] Here we make the link to oxidation catalysis using ODH of a terminal water at the aqueous rutile TiO_2 (110) interface as example. Applying a functional including a fraction of exact exchange (HSE06[11]) we find that localization reduces the oxidative power of a photo-generated hole by 0.6 V. However, viewed from an electrolysis perspective, this relaxation is crucial. Without it ODH of an adsorbed water molecule would require even higher potentials than ODH in solution. Our calculations also indicate that the net activation of ODH by the TiO_2 surface is almost entirely due to an increase of the acidity of an adsorbed water molecule. These results have been obtained from a DFT based molecular dynamics (DFTMD) simulation of a fully atomistic periodic slab model of

[*]To whom correspondence should be addressed
[†]University of Cambridge
[‡]University of Zurich
[¶]*Present address*: Johannes Gutenberg University Mainz
[§]*Present address*: Department of Materials, ETH Zurich

the interface (see Figure 1). A similar model system was used in preliminary DFTMD calculations of the acidity[12] and band edge energies[13] of the aqueous TiO_2 electrode.

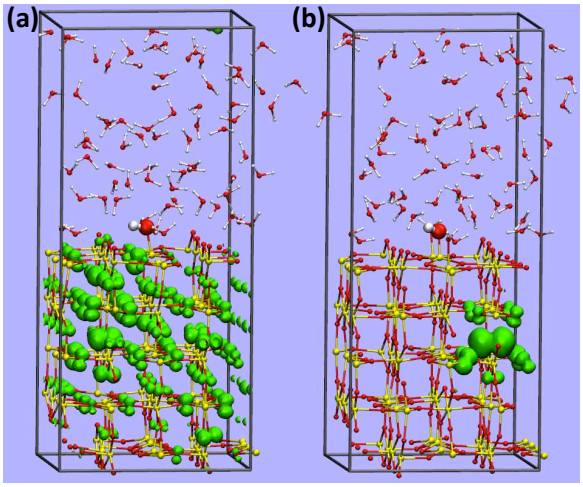

Figure 1: DFTMD model of a rutile TiO_2 (110) water interface from which a proton and electron has been removed. Ti, O and H atoms are represented in yellow, red and white, respectively. The highlighted surface hydroxide is the deprotonated water. The spin density of the electronic hole is visualized by green isosurfaces with the density of 5×10^{-4}. (a) and (b) are snapshots of MD trajectories generated using PBE and HSE06, respectively.

ODH is well-known in physical organic chemistry where it is the key process in proton coupled electron transfer (PCET).[14] For the analysis of the thermochemistry of a PCET reaction it has been found useful to resolve the reaction into a deprotonation and oxidation step.[14] This is visualized for our homogeneous reference reaction in the triangle diagram of Scheme 1a. Heterogeneous ODH will be subjected to a similar analysis. The dehydrogenation of terminal H_2O is written as

$$TiOH_2 \rightarrow TiOH^\bullet + H^+ + e^- \qquad (1)$$

and separated in a deprotonation and ionization

$$TiOH_2 \rightarrow TiOH^- + H^+ \qquad (2a)$$
$$TiOH^- \rightarrow TiOH^\bullet + e^- \qquad (2b)$$

where Ti stands for the five-fold coordinated Ti^{4+}_{5c} terminal site.[2] The link to photo-catalysis is made by introducing one further intermediate step. We assume that the electron is not taken directly from the surface OH^- group but from the valence band. This leaves a free hole h^+_f which must be trapped by the OH^- group to produce the surface $OH^\bullet$ radical. Reaction 2b is thus resolved as

$$TiOH^- \rightarrow TiOH^- + h^+_f + e^- \qquad (3a)$$
$$TiOH^- + h^+_f \rightarrow TiOH^\bullet \qquad (3b)$$

Charge and particle numbers are fixed in DFTMD simulations. The electronic charge of the model electrode and protonation state of the surface must therefore be matched to electrode potentials and pH in order to make meaningful comparison to electrochemical experiment. pH is a critical parameter for metal oxides. Because of the buildup of an electric double layer due to changes in protonation state ionization energies, such as the energy of reaction 2b, shift in response to changes in pH, even though protons are not directly involved in the reaction itself.[15] This complication is better avoided in a first atomistic simulation of heterogeneous ODH. Our reference state is therefore an electrode without excess or deficit charge, either electronic or protonic. This state corresponds to the flatband potential at the pH for which the net proton charge vanishes (PZC).

The experimental PZC of rutile TiO_2 (110) is about 5. The flatband potential at this pH is given in Ref. 15 as -0.25 V *vs* SHE. This potential is well below the threshold for water oxidation. The population of oxidized water residues ($OH^\bullet$, O)[3,4] can therefore safely assumed to be zero. Also ΔpK_a for rutile TiO_2 (110) surfaces is too high for dissociation of adsorbed water which would create ion pairs without a change of net surface charge.[12,16] Our reference model was therefore set up as a surface covered by water molecules only.

Free energies will be represented as reversible potentials *vs* SHE at PZC. The potential of the ODH reaction 1 must therefore be adjusted to the nonstandard concentation of the product H^+ with all other components at standard concentration. This quantity will be denoted by $U'_{\rm dh}$. Similarly, the free energy of reaction 2a, while not a redox reaction, will be given by an effective reversible deprotonation potential at PZC

$$eU'_{\rm dp} = 2.30 k_{\rm B}T\,(pK_a - pH_{\rm PZC}) \qquad (4)$$

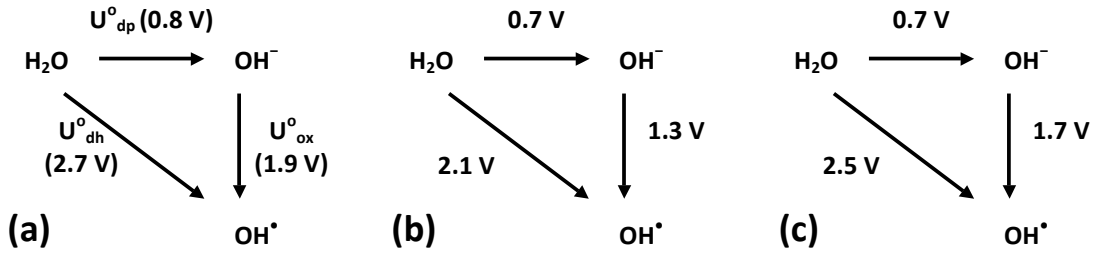

Scheme 1: Decomposition of oxidative dehydrogenation of water into deprotonation and oxidation reactions in solution. Standard reaction free energies (pH = 0) are represented as reversible electrode potentials *vs* SHE. (a) Experiment; (b) computed using BLYP; (c) computed using a hybrid functional HSE06.[11]

where pK_a is the intrinsic acidity of the terminal H_2O molecule and $pH_{PZC} = 5$. The oxidation 2b is a special case. While protons are not directly involved as reactant or product, the corrsponding potential U_{ox} is implicitly dependent on pH and its value at PZC will therefore be equally marked by a prime. Hess law then demands that the three potentials just defined satisfy

$$U'_{dh} = U'_{dp} + U'_{ox} \tag{5}$$

Eq. (5) also suggests an electrochemical interpretation for U'_{dp}, namely, the thermodynamic overpotential for deprotonation of a water molecule.

U'_{ox} in Eq. (5) in turn consists of two contributions, one from each of the reactions 3. The energy cost of reaction 3a is the ionization potential (IP) of the valence band at PZC, or in electrochemical terms, the SHE potential of the VBM referred to as U'_{VBM}. Therefore U'_{ox} can be decomposed as

$$eU'_{ox} = eU'_{VBM} + \Delta_{tr}G \tag{6}$$

where the hole trapping energy $\Delta_{tr}G$ is the free energy change of reaction 3b. The decomposition of heterogeneous ODH is summarized in the extended triangle diagram of Scheme 2(a).

To see why localization is crucial for the activation of ODH, we define a separate potential for the proton coupled formation energy of a *free* hole

$$U'_{dhf} = U'_{dp} + U'_{VBM} \tag{7}$$

The energies in Eq. (7) can be inferred from experimental data. Converting the VBM of Ref. 1 to the PZC using the linear relation given in Ref. 15 we obtain $U'_{VBM} = +2.65$V (we have taken the value for the dark). The intrinsic pK_a of a surface group is not directly accessible to experiment but can be estimated with the help of an empirical surface complexation model.[16] The popular MUSIC model of Ref. 16 assigns a p$K_a = 7.5$ to a terminal H_2O on rutile $TiO_2(110)$. This gives according to Eq. (4) an effective deprotonation potential of $U'_{dp} = 0.14$ V. Substituting in Eq. (7) we find $U'_{dhf} = 2.8$ V. Without self trapping ($\Delta_{tr}G < 0$) the oxidation potential for surface ODH of H_2O at PZC would be higher than the 2.4 V for ODH in solution. Hole localization is therefore necessary to offset the high energy of free holes in TiO_2.

The computational method is based on insertion of electrons and protons in extended model systems.[17] The key quantities in such schemes are vertical energy gaps computed as the cost in total energy of eliminating an electron (oxidation), proton (deprotonation) or both (dehydrogenation) keeping the coordinates of all common atoms fixed. In our DFTMD implementation[12,13,18] the vertical energy gaps are used as input for a free energy perturbation method giving the corresponding adiabatic ionization, deprotonation or dehydrogenation energies. These free energies are represented on a pK_a and SHE scale by comparing to the solvation free energy of the proton, which is computed from the deprotonation free energy of an hydronium (H_3O^+). The conversion to pK_a and SHE potentials requires corrections for translational entropy and proton zero point motion effects.[18,19] The thermochemical corrections used in the present calculation are summarized in the supporting information. Note that our method is developed to compute thermodynamic free energy changes other than activation energies. Born-Oppenheimer DFTMD and static geometry optimization calculations were

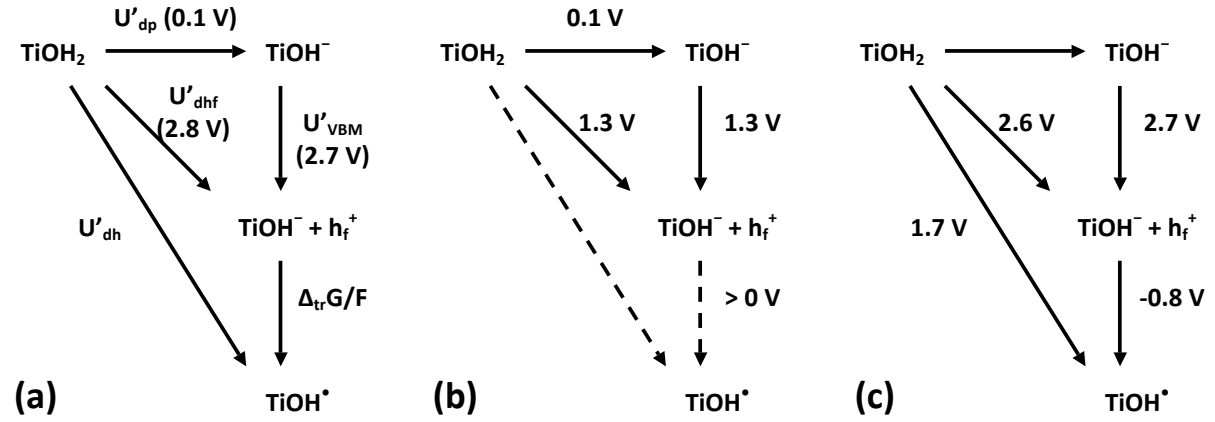

Scheme 2: (a) Extended thermodynamic triangle for heterogeneous ODH of water with a free valence band hole h_f^+ as intermediate (see reactions 3); (b) computed free energies from DFTMD/PBE; (c) HSE06[11] estimates from total energies and Kohn-Sham eigenvalue. Some experimental estimates are given in (a). Note that the pH is at PZC of TiO_2, different from Scheme 1 where the standard pH condition is used. The dashed arrows in (b) indicate that for PBE the free hole plus anion is the stable product.

carried out using the freely available program package CP2K/Quickstep.[20] Application of exact exchange functionals comes at a substantial increase in computational costs. Recent progress has been able to reduce these costs and the present simulation makes use of our latest implementation of such a scheme.[21]

The model system is shown in Figure 1. The system consists of a TiO_2 slab and a water layer replicated by 3D periodic boundary conditions. All components are treated at the same level of theory. The detailed specification of the model and DFTMD parameters are given in the supporting information. The model system for the homogeneous reference reaction is the "standard" 32 H_2O molecule cubic box. This is the system in the reduced state. The oxidized system contains one OH radical and 31 water molecules. Level alignment ("band offset") problems are avoided by always coupling removal of an electron with removal of a proton from the same supercell.

The computational SHE allows us to align the potentials of Schemes 1 and 2 with the band edges of the aqueous TiO_2 in one and the same level diagram. The result is shown in Figure 2. The solution redox levels and TiO_2 band edges are known experimentally. Comparison of the computed to the measured potentials is therefore a critical test of our approach. As can be seen from the data in Scheme 1 the GGA underestimates homogeneous $H_2O/OH^\bullet$ oxidation potential by as much as 0.6 V. The oxidation potential of OH^- shows a similar bias while the accuracy for the acid dissociation constant (pK_W) is significantly better. This mixed performance of the GGA is consistent with previous DFTMD calculations of homogeneous ODH redox energies.[18,19] We note that while limitations in length and time scale are critical issues in DFTMD simulations, these effects are of secondary importance compared to "intrinsic" inaccuracy of the GGA for ionization potentials in extended systems. One piece of evidence for this claim is that application of HSE06 reduces the error in ionization energies from 0.6 to 0.2 V approaching the overall uncertainty of DFTMD calculations (see supporting information for details).

The band edge positions at PZC give a very similar picture. The calculation was already carried out in Ref. 13. We found that PBE places the VBM an eV too high while the conduction band minimum (CBM) is almost perfectly aligned with experiment.[1,15] The band edges have been recomputed for the somewhat thicker solid slab used here (5 instead of 3 TiO_2 trilayers). The PBE results are $U'_{\mathrm{VBM}} = 1.45$ V *vs* SHE compared to 2.65 V in experiment and $U'_{\mathrm{CBM}} = -0.45$ V compared to -0.35 V. Again ionization energies are seriously underestimated at the GGA level. Application of HSE06 leads to a dramatic improvement for the VBM giving $U'_{\mathrm{VBM}} = 2.69$ V while marginally lift-

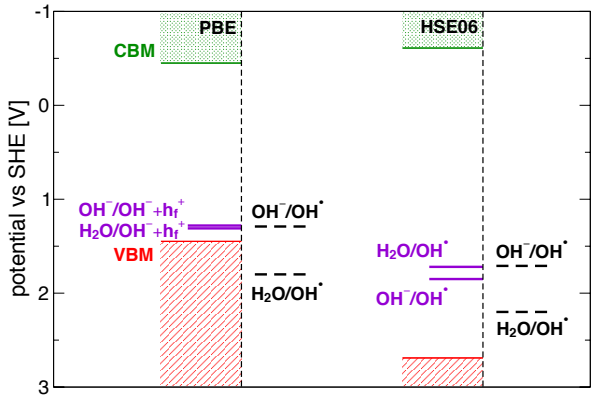

Figure 2: Alignment of the redox energy levels for ODH of water in solution (dashed lines), on the (110) surface of a rutile TiO_2 electrode (solid lines) and the valence band maximum (VBM) and conduction band minimum (CBM) of the aqueous electrode. GGA (left) and HSE06 results (right) have been taken from Scheme 2(b) and 2(c), respectively.

ing the CBM ($U'_{\mathrm{CBM}} = -0.61$ V). In view of the increased computational cost the HSE06 band edges were obtained from the HOMO and LUMO of a model system in which the solvent is replaced by a single monolayer of adsorbed water. For the reason of consistency the same approach was applied for the computation of the VBM and CBM for PBE. The justification for this simplification is given in the supporting information.

After the examination of the accuracy of the calculation of the reference energies in solution and the solid we are now ready to discuss the results for heterogeneous ODH. Comparing the VBM and surface redox potentials in Figure 2 we see that the gap between these levels is significantly larger for HSE06 than PBE. This is the effect of hole localization. This becomes evident when we analyze what happens if we remove a proton from a surface water and an electron from the solid electrode. If implemented in a PBE based simulation we are left with an hydroxide anion (OH^-) on the surface and a delocalized hole in the valence band of the solid as shown in the snapshot of Figure 1(a). The product we hoped to obtain, the hydroxyl ($OH^\bullet$) surface defect, never forms. The spurious stability of the free hole in the GGA was already noted in Refs. 7–10. Continuation of the PBE trajectory with HSE06 produced a hole localized in the bulk region of TiO_2 slab as shown in Figure 1(b). Recreating the localized hole in the simplified one water monolayer model system and taking the total energy difference relative to the free hole we find a hole trapping energy of $\Delta_{\mathrm{tr}}G = -0.57$ eV.

To produce a surface $OH^\bullet$ the bulk hole must oxidize the OH^- by localizing at the surface site where this anion resides. This gains us an additional 0.27 eV. With these energies as input we can compute the oxidation potential U'_{ox} of Eq. (6). The result is the $OH^-/OH^\bullet$ level at 1.85 V in Figure 2. The corresponding $H_2O/OH^\bullet$ level was computed from the energy for simultaneous removal of a proton and electron. Adjusting for the pH at PZC we obtained $U'_{\mathrm{dh}} = 1.7$ V. This should be compared to the $U'_{\mathrm{dh}} = 1.3$ V estimated from a full DFTMD simulation using PBE (see Scheme 2(b)). Recalling that in the PBE model the hole remains delocalized the 0.4 V difference in ODH potential is relatively modest. This is due to the complementary role of eU'_{VBM} and ΔG_{tr} in Eq. (6) leading to a compensation of errors.

In view of the difference in ODH product, it is somewhat surprising that GGA and HSE06 calculations seem to be in quantitative agreement on the net catalytic effect of the TiO_2 surface. Comparing the potentials in Schemes 1 and 2 and adjusting for the difference in pH, we find for PBE and HSE06 a decrease in U'_{dh} of 0.6 V and 0.5 V, respectively. Applying our PCET decomposition analysis reveals that the 0.5 V activation is almost entirely due to an increase in acidity of an adsorbed water. Compared to the values in solution, U'_{dp} is small in both model systems (0.07 V for PBE and -0.13 V for HSE06). The heterogeneous ODH potential is effectively determined by the cost of the oxidation of the OH^- anion. This cost is moreover the same on the surface and in the solution. The levels for oxidation of OH^- on the surface and in solution are aligned in left and right panel of Figure 2.

In summary, we have shown that self trapping of holes in TiO_2 plays an important but ambivalent role in the oxidative dehydrogenation of a terminal H_2O at the rutile (110) water interface. Localization decreases the oxidative power of photogenerated free holes by 0.6 V. On the other hand without localization the formation of surface hydroxyl radicals is not possible. The same effect also decreases the reversible potential for

electrolytic ODH. Separation in a deprotonation and ionization component suggests that TiO_2 in essence acts as a Lewis acid increasing the acidity of adsorbed water molecules. Adsorption has little effect on the cost for oxidation of OH^- to $OH^\bullet$. The cost remains as high as in bulk solution. One can therefore speculate that the lack of electronic activation is one of the reasons for the poor electro-catalytic properties of titania as reflected in the high overpotential.[22] These issues can be probably best resolved by repeating a similar PCET analysis for a good oxidation catalyst, in particular RuO_2. The ultimate aim would be to find a suitable electronic descriptor for water splitting which could provide an electronic structure basis for the chemisorption energy descriptor used in volcano plots.[5]

Keywords: Water oxidation, proton coupled electron transfer, density functional theory, free energy calculations

Acknowledgement

J. C. thanks Emmanuel College at Cambridge for research fellowship. Dr. Aron Cohen is acknowledged for helpful discussions about density functionals and the delocalization error. The calculations in this work have been performed using an allocation of computer time on HECToR, the UK's high-end computing resource funded by the Research Councils, as part of a grant to the UKCP consortium, and at the Swiss National Supercomputing Centre (CSCS).

Supporting Information Available

Supporting information for this article is available.

Notes and References

(1) Nozik, A. J.; Memming, R. *J. Phys. Chem.* **1996**, *100*, 13061–13078.

(2) Fujishima, A.; Zhang, X.; Tryk, D. A. *Surf. Sci. Rep.* **2008**, *63*, 515 – 582.

(3) Valdés, Á.; Qu, Z. W.; Kroes, G. J.; Rossmeisl, J.; Nørskov, J. K. *J. Phys. Chem. C* **2008**, *112*, 9872–9879.

(4) Li, Y.-F.; Liu, Z.-P.; Liu, L.; Gao, W. *J. Am. Chem. Soc.* **2010**, *132*, 13008–13015.

(5) Rossmeisl, J.; Qu, Z.-W.; Zhu, H.; Kroes, G.-J.; Norskov, J. K. *J. Electroanal. Chem.* **2007**, *607*, 83–89.

(6) Fang, Y.-H.; Liu, Z.-P. *J. Am. Chem. Soc.* **2010**, *132*, 18214–18222.

(7) Morgan, B. J.; Watson, G. W. *Phys. Rev. B* **2009**, *80*, 233102.

(8) Deskins, N. A.; Dupuis, M. *J. Phys. Chem. C* **2009**, *113*, 346–358.

(9) Valdés, Á.; Kroes, G.-J. *J. Phys. Chem. C* **2010**, *114*, 1701–1708.

(10) Di Valentin, C.; Selloni, A. *J. Phys. Chem. Lett.* **2011**, *2*, 2223–2228.

(11) Krukau, A. V.; Vydrov, O. A.; Izmaylov, A. F.; Scuseria, G. E. *J. Chem. Phys.* **2006**, *125*, 224106.

(12) Cheng, J.; Sprik, M. *J. Chem. Theory Comput.* **2010**, *6*, 880–889.

(13) Cheng, J.; Sprik, M. *Phys. Rev. B* **2010**, *82*, 081406.

(14) Warren, J. J.; Tronic, T. A.; Mayer, J. M. *Chem. Rev.* **2010**, *110*, 6961–7001.

(15) Kavan, L.; Grätzel, M.; Gilbert, S. E.; Klemenz, C.; Scheel, H. J. *J. Am. Chem. Soc.* **1996**, *118*, 6716–6723.

(16) Hiemstra, T.; Venema, P.; Riemsdijk, W. *J. Colloid Interface Sci.* **1996**, *184*, 680 – 692.

(17) Rossmeisl, J.; Skúlason, E.; Björketun, M. E.; Tripkovic, V.; Nørskov, J. K. *Chem. Phys. Lett.* **2008**, *466*, 68 – 71.

(18) Cheng, J.; Sulpizi, M.; Sprik, M. *J. Chem. Phys.* **2009**, *131*, 154504.

(19) Costanzo, F.; Sulpizi, M.; Valle, R. G. D.; Sprik, M. *J. Chem. Phys.* **2011**, *134*, 244508.

(20) The CP2K developers group website: http://cp2k.berlios.de.

(21) Guidon, M.; Hutter, J.; VandeVondele, J. *J. Chem. Theory Comput.* **2010**, *6*, 2348–2364.

(22) Nozik, A. J. *Nature* **1975**, *257*, 383–386.